

Polarization of Pb Vapor.

I. Orientation of the 3P_0 Ground State of Pb^{207}

Hyatt M. Gibbs and Berken Chang*

Bell Telephone Laboratories, Murray Hill, New Jersey 07974

and

Rodney C. Greenhow†

Physics Department, University of California, Berkeley, California

(Received 14 July 1969)

The method of optical pumping of diamagnetic atoms with zero orbital angular momentum (1S_0) has been extended to an atom with nonzero orbital angular momentum (3P_0), yielding $|\mu_I|_{\text{uncorrected}} = 0.5726(6) \mu_N$. An expression for the signal is found and the complications of branching to the metastables are discussed. The apparatus is described.

1. INTRODUCTION

The technique of optical pumping¹ has been successfully applied to a large number of free atoms in diamagnetic ground states with no orbital angular momentum, i. e., 1S_0 states.² High-precision determinations of nuclear moments have been possible since the nuclear Zeeman effect is not masked by a much larger hyperfine interaction. In addition, the free-atom measurements suffer no chemical shift. Of equal interest, optical pumping has permitted a direct observation of the relaxation of the nuclear polarization.³

This paper reports the extension of this 1S_0 optical pumping technique to a diamagnetic state with nonzero orbital angular momentum, in particular, the 3P_0 ground state of Pb^{207} .⁴ The present measurement of the nuclear moment of Pb^{207} demonstrates the applicability of the technique to precision determinations of the moments of 3P_0 atoms. The surprising resistance to relaxation of the nuclear polarization of the 3P_0 state is also discussed.

The theoretical expression for the signal is derived in Sec. 2. The apparatus is described in Sec. 3. The data are presented and discussed in Sec. 4. Earlier aspects of this work have been presented previously.^{4,5}

2. THEORY

A. Orientation Signal

A theoretical expression for the signal is desired for the following experiment. Pb^{207} ($I = \frac{1}{2}$) atoms in the 3P_0 ground state are situated in a static magnetic field of a few hundred G. Their density n is sufficient to absorb a small portion of the incident pumping light intensity consisting of the two 2833 Å hyperfine components A_- and A_+ (see Fig. 1). The static field, incident radiation, and quantization axis are collinear. There are then two ground-

state sublevels with populations n_+ and n_- , where the signs refer to $M_F = \pm \frac{1}{2}$. n_+ and n_- are assumed equal in the absence of optical pumping since the latter produces a polarization much larger than that of the Maxwell-Boltzmann distribution. Expressions are desired for the equilibrium optically pumped orientation $(n_+ - n_-)/n$ and for the change in transmitted light intensity when the sample is disoriented by a resonant transverse radio frequency field.

Define T_1 as the relaxation time between the ground-state Zeeman sublevels. The transition probabilities for absorption of right circularly polarized light are proportional to the matrix elements $|[F'M' | er(1,1) | FM]|^2$, where $er(1,1)$ is one spherical tensor component of the electric dipole moment of the Pb atom.⁶ The relative values are given in Fig. 1. Let C be a constant such that $Cn_-(2A_- + A_+)$ is the absorption by n_- , and

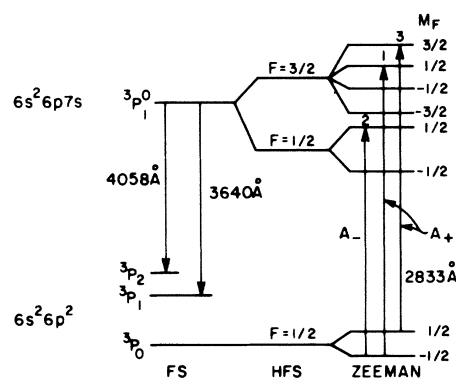


FIG. 1. Energy levels of Pb^{207} ($I = \frac{1}{2}$) relevant to optically pumping the 3P_0 ground state. The number above each arrowhead is the relative absorption transition probability for right circularly polarized light ($\Delta M_F = +1$).

Cn_+3A_+ is the absorption by n_+ . Assume that once the atom is in the excited state it has a probability k of returning directly to the ground state without any collisional depolarization, and $1-k$ of being depolarized by excited-state collisions or by fluorescing to a metastable state. In the latter case, assume no orientation remains when the atoms are deexcited to the ground state. The relative reemission probabilities to the ground state are shown in Fig. 2. The time evolution of n_+ is then

$$\begin{aligned} \dot{n}_+ - \dot{n}_- = & -(n_+ - \frac{1}{2}n)/T_1 && \text{relaxation} \\ & - Cn_+3A_+ && \text{absorption} \\ & + C[n_-(2A_- + A_+) + n_+3A_+] \frac{1}{2}(1-k) && \\ & && \text{metastable de-} \\ & && \text{excitation} \\ & + C\{2A_-n_-\frac{1}{3} + A_+n_-\frac{2}{3} + 3A_+n_+\}k, && \\ & && \text{reemission} \quad (1) \end{aligned}$$

where T_1 is the longitudinal relaxation time.³ With $n_{\pm} = \frac{1}{2}[n_{\pm}(n_+ - n_-)]$, Eq. (1) becomes

$$\begin{aligned} \dot{n}_+ - \dot{n}_- = & -(n_+ - n_-)(1/T_1 + 1/T_p) \\ & + nC[A_- - A_+ - \frac{1}{3}k(A_- - 5A_+)], \quad (2) \end{aligned}$$

where the pumping time T_p is defined by

$$T_p^{-1} = [A_- + 2A_+ - \frac{1}{3}k(A_- + 4A_+)]C. \quad (3)$$

The equilibrium polarization P is found from (2) with $\dot{n}_+ - \dot{n}_- = 0$:

$$P \equiv (n_+ - n_-)/n = [A_- - A_+ - \frac{1}{3}k(A_- - 5A_+)]C$$

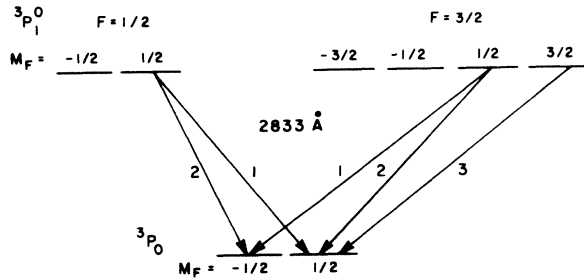


FIG. 2. Reemission transition probabilities. The relative probabilities for reemission from the $^3P_1^0$ excited state to the 3P_0 ground state are given beside the transition arrows.

$$\times (1/T_1 + 1/T_p)^{-1}. \quad (4)$$

A signal can now be defined as the change in absorption when the optically produced orientation P is destroyed by a resonant rf field:

$$S \equiv \alpha(P=0) - \alpha(P). \quad (5)$$

It will be found convenient later to divide the signal into its two resolvable hyperfine components [the total absorption of A_+ is $\alpha_+ = CA_+(n_- + 3n_+)$; similarly, $\alpha_- = 2CA_-n_-$]:

$$\begin{aligned} S_+ &= \alpha_+(P=0) - \alpha_+(P) \\ &= CA_+(2n_- - n_+ - 3n_+) = -nCA_+P, \quad (6) \end{aligned}$$

$$\begin{aligned} S_- &= \alpha_-(P=0) - \alpha_-(P) \\ &= 2CA_-(\frac{1}{2}n - n_-) = nCA_-P, \quad (7) \end{aligned}$$

$$S = S_+ + S_- = nCP(A_- - A_+), \quad (8)$$

$$\begin{aligned} S &= nC^2(A_- - A_+)[A_- - A_+ - \frac{1}{3}k(A_- - 5A_+)] \\ &\times (1/T_1 + 1/T_p) \quad (9) \end{aligned}$$

B. Discussion

It is immediately clear from (9) that the signal vanishes for a hyperfine light-intensity ratio A_-/A_+ equal to 1 or $(3-k)/(3-5k)$. In addition, it is very small in the region between these two zeros, as seen in Fig. 3. The values of k were chosen as follows: $k=1$ corresponds to no branching to the metastables and no excited-state disorientation (the case for the 1S_0 states previously pumped), $k=0.27$ is the measured⁷ branching to the ground state with no excited-state mixing, and $k=0$ is the case for complete disorientation in the excited state for arbitrary branching (since disorientation in the excited state is assumed equivalent to disorientation in the metastable state). For an evacuated cell, k is expected to be 0.27, for which the signal very nearly vanishes for $A_-/A_+ = 0.5-1.0$. Unfortunately, the ratio from most lamps falls in this region. The theoretically expected ratio with no self-reversal is $A_-/A_+ = 0.5$. Most lamps emit more useful light when some self-reversal is permitted; A_-/A_+ then increases since A_+ is absorbed more strongly than A_- . Often the maximum output is achieved when these components are equal.⁸ The signal is also small for $A_-/A_+ = 0.5-1.0$ in the case of complete excited-state disorientation. In addition, a high density of buffer gas was avoided in the early work because of the fear that the excited-state hyperfine coupling might be broken. This coupling is essential to orientation of the nucleus:

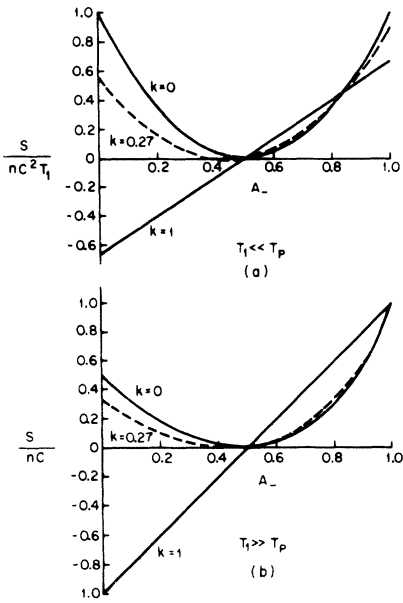


FIG. 3. Signal strength versus the hyperfine component A_- of the pumping light with the branching ratio k to the ground state as parameter. The light is normalized such that $A_- + A_+ = 1$. See Eq. (9).

The angular momentum of the polarized light is transferred to the electron by optical absorption and to the nucleus by the electron-nuclear hyperfine interaction.

Another approach to enhance the signal is to insert a hyperfine filter between the lamp and cell to eliminate one of the hyperfine components. Large signals would then result; see Fig. 3, with $A_- = 0$ or 1. However, the insertion of such a filter (described in Sec. 3) results in an order-of-magnitude reduction in the transmitted light. Taking the hint from the work on optically pumping Sr^+ ions,⁹ the possibility of placing the filter between the cell and detector was investigated. If

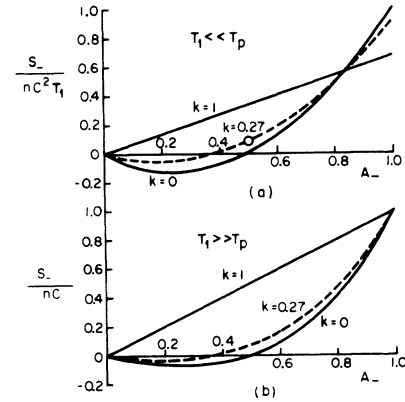


FIG. 4. Strength of the hyperfine component S_- of the transmitted signal as a function of A_- with $A_- + A_+ = 1$. The circle indicates the approximate operating condition for most of the resonances used in the moment determination. See Eq. (7).

there were no metastable branching or excited-state disorientation (i. e., $k = 1$), such a placement would be preferred since both hyperfine components pump in the same sense and the pumping time would be minimized. It is shown in Fig. 4 that, even for the Pb case of $k = 0.27$, reasonably large signals are predicted for the readily attainable values $A_-/A_+ = 0.67-1.0$ ($A_- = 0.4-0.5$, for $A_- + A_+ = 1$) provided only the hyperfine component S_- of the signal is observed. The signal was first observed and most of the data taken under these conditions; variations are discussed in the following paper.

C. Linewidth

So far, the discussion has been limited to the magnitude and sign of the signal. For negligible inhomogeneity in the static field H_0 and low intensity, the polarization as a function of rf field H_1 is³

$$P = P_0 \left[1 - \left(\frac{T_1}{T_2} \gamma^2 H_1^2 / \pi^2 \right) \left((\nu - \nu_0)^2 + \frac{1}{\pi^2 T_2^2} + \frac{\gamma^2 H_1^2 T_1}{\pi^2 T_2} \right)^{-1} \right] = A \left[1 + \left(\frac{\nu - \nu_0}{\frac{1}{2} L} \right)^2 \right]^{-1} + B, \quad (10)$$

where ν is the frequency of H_1 , $\gamma H_0 = \nu_0$; and T_1 and T_2 are the longitudinal and transverse relaxation times. The full width at half-maximum L is then defined by

$$L^2 = (\pi T_2)^{-2} + (\gamma/\pi)^2 (T_1/T_2) H_1^2. \quad (11)$$

A Lorentzian fit to the data can then be used to place a lower limit on T_2 if it is too long to produce sufficient broadening to be detected in the presence of inhomogeneous field broadening. Information on T_1 is much more difficult to obtain by linewidth methods, but usually $T_2 \leq T_1$. Some indication of the value of T_1 can be gained from the magnitude of the signal but this is obscured by the spectral profile, as discussed in Sec. 2A and 2B.

3. APPARATUS

The block diagram of the experimental apparatus is shown in Fig. 5. The components are described briefly below.

A. Lamp

The most crucial component in this (and most) optical pumping experiment is the source of resonance radiation. A flow lamp similar to that developed at Columbia,¹⁰ but excited by microwaves, was found to produce 5 or 10 times more fluorescence in a cell of Pb vapor than an electrodeless lamp. Similar results have been reported by Saloman and Happer.⁷ Churchill has developed a flow lamp of simpler and sturdier construction, which operates for days without attention. The 0.015-in. molybdenum filament delivers 500 W for weeks before failing. Details of the construction and operation will soon be available.¹¹

B. Circular Polarizer

Since the nuclear spin of Pb^{207} is $\frac{1}{2}$, no alignment¹² is produced by unpolarized light. The production of an orientation¹² requires elliptically polarized light. A Polacoat PL-40 linear polarizer¹³ ($\approx 20\%$ transmission at 2833 \AA) and a stressed quartz quarter-wave plate¹⁴ suffice for an effective circular polarizer.

C. Cells

The Suprasil quartz absorption cells were constructed by Pyrocell.¹⁵ The cells were not cleaned in any way before use. A few tens of milligrams of Pb^{207} -separated isotope¹⁶ were placed (in air) in a sidearm which was then attached to the cell through a 1-cm-long $\times 1$ -mm-diam capillary. The cell was attached to the vacuum system through a 5-cm-long $\times 1$ -mm-diam capillary. Resonances were studied in two cylindrical cells: 3 cm diam $\times 5$ cm long and 1.8 cm diam $\times 2.5$ cm long.

D. Static Magnetic Field

A constant magnetic field of 100–500 G was obtained from a set of coils manufactured by Eastern Scientific Instruments. The water-cooled coils are alternate layers of aluminum and Mylar encased in epoxy with an inside diameter of 25.5 cm. Their configuration is intermediate between Helmholtz and solenoid. A Hewlett-Packard 6269A power supply provided the approximately 10.4 G/A with better than 0.1% stability over several hours.

E. Oven

The oven, mounted inside the static-field coils, consists of a 15-cm-diam $\times 12.5$ -cm-long water-cooled shell, insulated by Cerafelt (Johns-Manville) from a hollowed out 10-cm-diam $\times 10$ -cm-long copper cylinder. An American Standard BXA1-

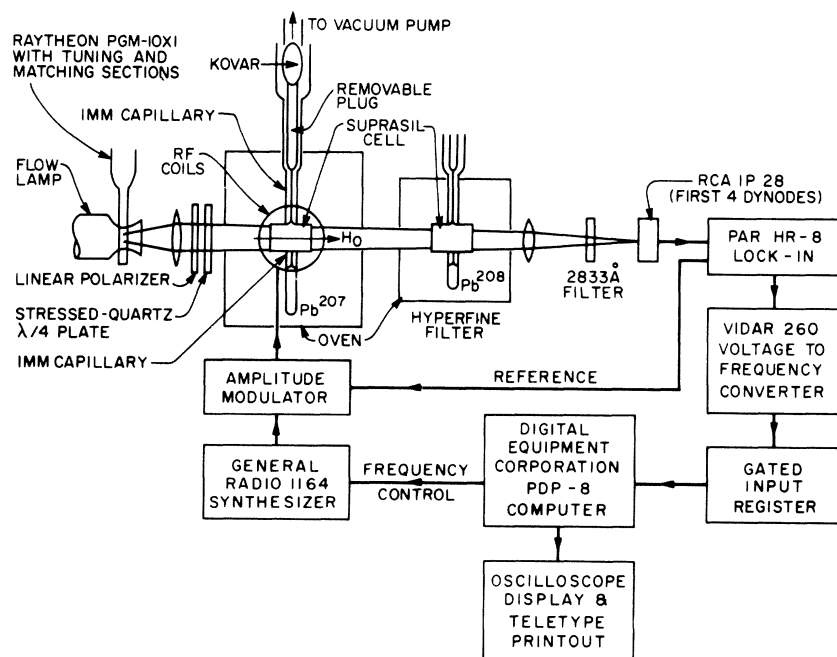


FIG. 5. Block diagram of the experimental apparatus.

B50-11.5M heater is wrapped around each end of the copper cylinder, which is divided in half for easy insertion of resonance cells. Only nonmagnetic materials were used in constructing the oven. The field produced by the heaters is about 30 mG at the highest temperature attained, 725 °C. A BXA1-B18-12M heater was used around the top capillary and the sidearm. The top, cell, and sidearm temperatures were monitored by Pt-10% Rh thermocouples.

F. rf Field

Inside the copper cylinder are situated the two rf coils, each of four rectangular (5×7 cm) turns of 1-mm-diam silver wire. The radio frequency was generated by a digitally controlled General Radio 1164 frequency synthesizer, amplitude modulated¹⁷ at 10–250 Hz for phase-sensitive detection, stepped down by a factor of about 150 by a transformer, amplified by a General Radio 1233-A, further amplified by a Krohn-Hite DCA-50R, and impedance matched to the coil by a Krohn-Hite MT-56. This system produced a linearly oscillating field with peak amplitude H_1 of about 20 G. After the resonance was found, fields of 10–1000 mG were used; the Bloch-Siegert¹⁸ shift ($H_1/2H_0$)² was then less than 10^{-4} at all times, i. e., negligible.

G. Hyperfine Filter

The purpose of the hyperfine filter is to absorb most of the light emitted from $^3P_1^o$ ($F = \frac{3}{2}$) to 3P_0 ($F = \frac{1}{2}$), labeled A_+ in Sec. 2A and Fig. 1, while transmitting most of the $^3P_1^o$ ($F = \frac{1}{2}$) to 3P_0 ($F = \frac{1}{2}$) light A_- . Figure 6(a) displays both the theoretical peak intensities¹⁹ expected for a natural lead lamp and the observed spectral profile which is broadened by the Doppler effect, self-reversal in the lamp, and by the instrumental width of the Fabry-Perot interferometer.²⁰ This profile immediately suggests the use of a pressure-shifted absorption cell to eliminate A_+ in a manner similar to that employed in other elements.²¹ That this should work was substantiated by much earlier work by Clayton and Ch'en²² giving a shift for Pb 2833 Å as 0.188 cm^{-1} (violet) per unit relative density of helium. They do not report the broadening for Pb, but for Ag the broadening is greater than the shift.

The hyperfine filter consists of a 3-cm-diam \times 5-cm-long quartz cell (with capillaries like the resonance cells) heated to 650 °C. The sidearm containing the Pb^{208} isotope²³ was situated in the thermal gradient between the heaters and water-cooled shell; its temperature was probably about 550 °C. The absorption by the Pb^{208} without helium is shown in Fig. 6(b). The addition of 400 Torr of He (measured on a room-temperature gauge in communication with the hyperfine-filter absorption

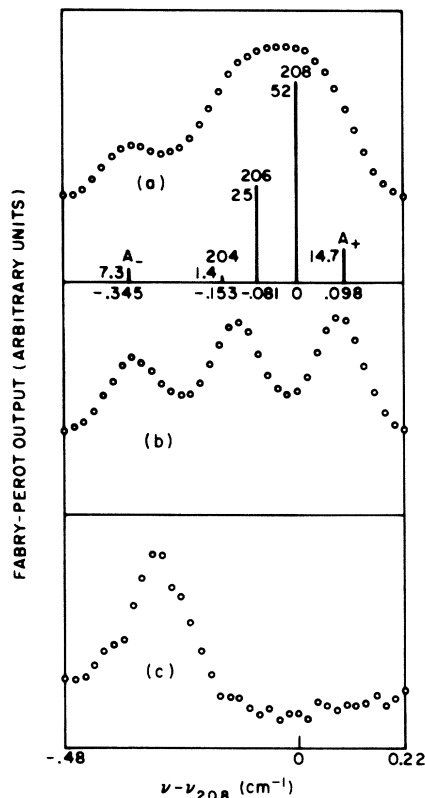


FIG. 6. Fabry-Perot spectral scans demonstrating the efficacy of the hyperfine filter. The three curves have different vertical scales. The apparent shift of A_- in (c) from (a) and (b) is believed to be instrumental. (a) Profile of natural Pb lamp with cold hyperfine filter. The maximum intensities expected from isotopic abundance and assuming no self-reversal are shown by the vertical lines. (b) Pb^{208} absorption by hyperfine filter cell at 675 °C (Pb^{208} in sidearm was probably under 600 °C). (c) Same as (b) with the addition of 400 Torr of He.

cell) shifts and broadens the Pb^{208} absorption resulting in Fig. 6(c). The shift is expected to be only 0.03 cm^{-1} compared with the 0.098 cm^{-1} difference between the Pb^{208} peak absorption and A_+ ; apparently the broadening is somewhat greater.

The helium diffuses through the hot quartz cell in a few days; the 1-liter helium flask left open to the cell served as a ballast.

H. Data Averager

The averaging system was designed for day-long runs in order to search effectively for very small signals. The basic idea is by now rather standard. One obtains long-term averaging by sweeping through the resonance repetitively. In this case, the Digital Equipment Corporation PDP-8 computer

provides the necessary memory. In addition, it is much more flexible than conventional pulse-height analyzers. Some of the features incorporated in the present system which are often absent from hard-wired averagers are: choice of any number of channels from 1 to 200 (many more if data reduction routines are eliminated); stop or print-continue or print-clear-continue after any number of cycles between 1 and 4095; option to subtract background after each cycle; up-only or up-down scanning option; 12-bit analog control (for example, Fabry-Perot) or 27-relay digital control (for example, synthesizer) of external devices; stop at completion of current cycle when any channel is filled; simultaneous display of both groups; subtraction of one curve from another; neat permanent digital (teletype) and visual (oscilloscope photograph) record of each run if desired; and display of all channels while accumulating (this is very helpful when the time per channel is longer than 0.1 sec). The greatest advantage of a computer system is its ability to analyze data on line. In the present experiment, a least-squares Lorentzian program determines the best-fit values and uncertainties of the background, peak, center frequency, and width [see Eq. (10)]. This program typically takes 10–20 sec for 25 channels and can be used while accumulating new data in the other group. Immediate data analysis is not only convenient but also saves time by permitting immediate reinvestigation of questionable results and further scrutiny of unexpected trends.

I. Detector

The 2833 Å transmission was monitored with a 1P28 photomultiplier tube. Use of only the first four dynodes yielded good secondary emission statistics at each dynode without saturation. A 2800 Å filter with a 125 Å half-width discriminated against some of the background light.

4. DATA

A. Detection and Relaxation of Orientation

One of the resonances obtained with the system of Fig. 5 is shown in Fig. 7. It was observed in an evacuated cell with the hyperfine filter, operating, as in Fig. 6(c), between the cell and detector. This corresponds approximately to the operating condition of the circle in Fig. 4(a).

The linewidth at low rf power can be used to place a lower limit on the average number of wall collisions N required to disorient the nuclear spin. A lower limit on the transverse relaxation time T_2 is given by [see Eq. (11)]

$$T_2 \geq (\pi L)^{-1}, \quad (12)$$

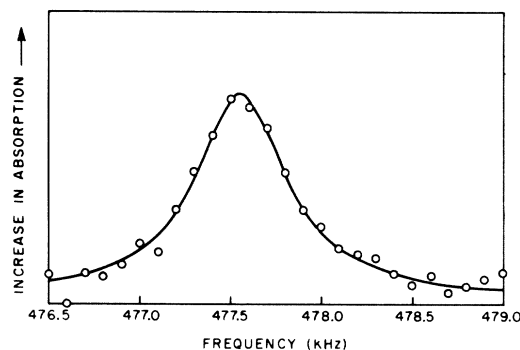


FIG. 7. Pb 3P_0 ground-state optical pumping resonance. This is one of the resonances used in the determination of the moment (see Table I). The proton resonance frequency was 2.3298 MHz (547.2 G). The best-fit parameters for a theoretical curve (solid) of the form of Eq. (10) are: amplitude $A = (5.524 \pm 0.176) \times 10^6$, background $B = (0.192 \pm 0.111) \times 10^6$, center frequency $\nu_0 = (477558.6 \pm 9.2)$ Hz, and width $L = (613.0 \pm 40.0)$ Hz.

where L is the full width of the resonance at half-maximum.³ The mean time of flight T_v between two wall collisions is

$$T_v = (4/\bar{v})(V/S), \quad (13)$$

where \bar{v} is the mean thermal speed and V and S are the volume and area, respectively, of the cell.²⁴ Assuming that the dwell time on the wall is short compared to the flight time and that $T_1 \geq T_2$, the average number of wall collisions required to disorient the nuclear spin is

$$N \equiv T_1/T_v \geq \bar{v}S/4\pi LV. \quad (14)$$

Linewidths as narrow as 250 and 500 Hz have been observed in the large and small cells, respectively; this implies that N must be greater than 16 and 14, respectively. The probability for nuclear-spin relaxation in a single-wall collision is then low for the 3P_0 state of Pb. This is in contrast to the alkali $^2S_{1/2}$ case where practically every collision completely disorients the electronic spin.²⁴ In buffer-gas collisions, the alkali 2P excited states relax much more rapidly than the $^2S_{1/2}$ ground state. This fact has led some authors to emphasize the importance of zero orbital angular momentum in achieving long relaxation times. It has also led to informal predictions of failure for any attempts to optically pump the 3P_0 state of Pb since its orbital angular momentum is nonzero. This work demonstrates unequivocally that the nuclear orientation of an atom with nonzero orbital angular momentum but with zero total electronic angular momentum \vec{J} can relax very slowly. This

is even more dramatically illustrated by the failure of 400 Torr of any of the rare gases to produce appreciable depolarization, as discussed in the following paper. The physical argument for expecting slow relaxation in the 3P_0 state has been given previously.⁴ In the evacuated case, one would not be surprised if the relaxation were rapid since a long dwell time on the wall would ensure complete depolarization. But, as in the Hg 1S_0 case, the dwell time is sufficiently short that the depolarization probability per wall collision is much less than unity.

B. Nuclear Moment of Pb^{207}

The technique described above for optically pumping the 3P_0 ground state of Pb^{207} has been applied to a precision determination of the nuclear moment. The uncorrected moment $|\mu_I|_{\text{uncorrected}}$ is given by

$$|\mu_I|_{\text{uncorrected}} = I h \nu / H_0,$$

where $I = \frac{1}{2}$, ν is the resonance center frequency, and H_0 is the magnetic field. The principle of the measurement was to alternately determine the resonance frequency by optical pumping and determine the magnetic field by proton resonance with a Magnion G-502 NMR Gaussmeter and Hewlett-Packard 5245L Counter. A bellows in the vacuum line between the pump and cell permitted placement of the NMR probe in the position of the cell.

More than an hour was required for the oven to cool or heat between the frequency measurement (600 °C) and the field measurement (25 °C). The oven was constructed of nonmagnetic materials to avoid a change in field with temperature. No shift in the NMR resonance occurs if the cold oven is removed. That the current in the heaters make no contribution has been verified by noting no shift in the NMR resonance when the heaters are on. Nor is a shift observed in the optical pumping resonance when the heaters are turned off. All other conditions of the experimental equipment were the same for the frequency and field measurements.

Data were taken in both the small and large cells, in magnetic fields of 350 and 500 G, with left and with right circularly polarized light, and for a range of rf-field intensities. None of these changes in experimental conditions noticeably affected the deduced moment.

The data and final results are summarized in Table I, yielding $|\mu_I(Pb^{207})|_{\text{uncorrected}} = 0.5726(6) \mu_N$, where the error is determined by linewidth limitations and lack of confidence in the field measurement. See Fig. 7 for one of the resonances used in the moment measurement.

ACKNOWLEDGMENTS

The authors would like to thank G. G. Churchill for excellent technical assistance. Many others have contributed to this research at various stages. In Berkeley, Dr. L. C. Bradley, III, and Pro-

TABLE I. Summary of nuclear moment data. Below is a summary of the final data used in the measurement of the nuclear moment of Pb^{207} ($I = \frac{1}{2}$). The first column lists the value of the proton resonance frequency ν_P assigned to the Pb^{207} frequency ν_I listed in the second column, yielding the nuclear moment of the third column. The actual measurements of ν_P are listed before and after each group of ν_I determinations. The uncertainty given for each ν_I is one-half the full width of the resonance curve at half-maximum. The uncertainty in ν_I from the least-squares fit is no larger than 10% of the uncertainty listed below. The uncertainty in the width is less than 20% of the width in every case.

Assigned ν_P	$\nu_I(Pb^{207})$	$ \mu_I /\mu_N = 2.79268\nu_I/\nu_P$
$\nu_P = 1.4923$ MHz		
1.4923	306.01 ± 0.17	0.57266
1.4929	306.10 ± 0.15	0.57260
1.4935	306.15 ± 0.20	0.57247
$\nu_P = 1.4935$ MHz. After field reversal and increase, $\nu_P = 2.3295$ MHz		
2.3298	477.55 ± 0.30	0.57244
2.3298	477.53 ± 0.30	0.57241
$\nu_P = 2.3300$ MHz. After replacing the large cell by the small one, $\nu_P = 2.2270$ MHz		
2.2270	456.72 ± 0.35	0.57273
2.2275	456.75 ± 0.5	0.57264
$\nu_P = 2.2275$ MHz		
Weighted average		0.57257

fessor S. P. Davis, Professor R. J. Hull, and Professor H. A. Shugart helped formulate and initiate the study. Professor W. Happer, Professor A. Lurio, and Professor M. N. McDermott have shared valuable information on techniques. Dr. C. W. White and Dr. M. Leventhal contributed

to the moment measurement. R. L. Youngs and G. J. Gass have helped design and construct apparatus. Finally, one of us (B.C.) is indebted to NASA for support at Berkeley and during the writing of the paper.

*Presently an NRC Postdoctoral Research Associate at NASA, Ames Research Center, Moffett Field, Calif.

†Present address: Physics Department, University of York, Heslington, York, England.

¹Recent reviews of the optical pumping technique are given by F. G. Major, in Atomic Interactions, edited by B. Bederson and W. L. Fite (Academic Press Inc., New York, 1968), Part B; B. Budick, in Advances in Atomic and Molecular Physics, edited by D. R. Bates and I. Estermann (Academic Press Inc., New York, 1967), Vol. 3; C. Cohen-Tannoudji and A. Kastler, in Progress in Optics, edited by E. Wolf (North-Holland Publishing Co., Amsterdam, 1966), Vol. V.

²(Hg), B. Cagnac, J. Brosnel, and A. Kastler, Compt. Rend. **246**, 1827 (1958); (He), F. D. Colegrove, L. D. Scheerer, and G. K. Walters, Phys. Rev. **132**, 2561 (1963); (Cd), J. C. Lehmann and J. Brosnel, Compt. Rend. **258**, 869 (1964); and J. C. Lehmann, J. Phys. **25**, 809 (1964); (Ba), L. Olschewski and E.-W. Otten, Z. Physik **196**, 77 (1966); (Yb), L. Olschewski and E.-W. Otten, ibid. **200**, 224 (1967); (Zn), P. W. Spence and M. N. McDermott, Phys. Letters **24A**, 430 (1967).

³Relaxation of Hg¹⁹⁹ and Hg²⁰¹ in evacuated cells has been studied carefully by B. Cagnac, Ann. Phys. (Paris) **6**, 467 (1961).

⁴H. M. Gibbs, B. Chang, and R. C. Greenhow, Phys. Rev. Letters **22**, 270 (1969). This is believed to be the first optical pumping of a *diamagnetic* state with nonzero orbital angular momentum; optical pumping of *paramagnetic* states with orbital angular momentum $L = 1$ has been reported: (Hg), J. P. Barrat, B. Chéron, and J. L. Cojan, Compt. Rend. Acad. Sci. **259**, 3475 (1964); (Xe), T. Hadeishi and C.-H. Liu, University of California Lawrence Radiation Laboratory Report No. UCLR-17667, 1967; (unpublished); (Ne), L. D. Scheerer, Phys. Rev. Letters **21**, 660 (1968); (Pb), H. M. Gibbs and B. Chang, Bull. Am. Phys. Soc. **13**, 1674 (1968).

⁵B. Chang, Ph.D. thesis, University of California Report No. 17765, 1967 (unpublished).

⁶A. R. Edmonds, Angular Momentum in Quantum Mechanics (Princeton University Press, Princeton, N. J., 1957), p. 68.

⁷E. B. Saloman and W. Happer, Phys. Rev. **144**, 7 (1966).

⁸The resolution of the Fabry-Perot interferometer used here is insufficient to verify this carefully for Pb, but such was the case for Rb: H. M. Gibbs and R. J. Hull, Phys. Rev. **153**, 132 (1967).

⁹H. Ackermann, G. zu Putlitz, and E. W. Weber, Phys.

Letters **24A**, 567 (1967).

¹⁰B. Budick, R. Novick, and A. Lurio, Appl. Opt. **4**, 229 (1965).

¹¹For a description of the construction of the flow lamp used here, write G. Churchill, Bell Telephone Laboratories, Murray Hill, N. J.

¹²For a discussion of alignment (nonvanishing quadrupole moment) and orientation (nonvanishing dipole moment) see W. Happer and E. B. Saloman, Phys. Rev. **160**, 23 (1967).

¹³From Polacoat Inc., Blue Ash, Ohio; see M. N. McDermott and R. Novick, J. Opt. Soc. Am. **51**, 1008 (1961).

¹⁴See Ref. 5, pp. 55-56.

¹⁵Westwood, N. J.

¹⁶92.4% Pb²⁰⁷, 5.48% Pb²⁰⁸, and 2.16% Pb²⁰⁶ from Union Carbide Corp., Oak Ridge.

¹⁷Square-wave modulator using field effect transistors designed by G. L. Tater, General Radio.

¹⁸F. Bloch and A. Siegert, Phys. Rev. **57**, 522 (1940).

¹⁹T. E. Manning, C. E. Anderson, and W. W. Watson, Phys. Rev. **78**, 417 (1950).

²⁰Fabry-Perot interferometer: 5-cm-diam fused silica plates, flat to $\lambda/200$ at 6000 Å, from Lambda Optics, Berkeley Heights, N. J.; dielectric coating with 11% transmission at 2833 Å by Perkin Elmer, Wilton, Conn.; piezoelectrically scanned etalon (developed by L. Moltenauer) from C. D. Grandt, 2709 Las Aromas, Oakland, California; plate spacing 0.7 cm; pinhole (0.053 cm diam) at focal plane of 30-cm lens and at the entrance slit of a monochromator (both slits 0.0125 cm; 1P28 detector). The finesse from the combined effects of nonflatness and imperfect reflection is calculated to be about 18 [see, for example, S. P. Davis, Appl. Opt. **2**, 727 (1963)]. The Doppler absorption width of 0.05 cm⁻¹ should then appear more like 0.1 cm⁻¹ in agreement with observation (through the best 1-cm-diam portion of the plates). A finesse measurement was not made. The spectral profile could be observed on an oscilloscope with at least a signal-to-noise ratio of 10 (through the apparatus, without the linear polarizer, and with the hyperfine filter cold). The use of a scanning Fabry-Perot is discussed in P. Jacquinet, Rept. Progr. Phys. **23**, 267 (1960).

²¹The use of a Rb hyperfine filter is described and earlier references given in Ref. 8.

²²E. D. Clayton and S. Ch'en, Phys. Rev. **85**, 68 (1952).

²³99.47% Pb²⁰⁸, 0.41% Pb²⁰⁷, 0.12% Pb²⁰⁶.

²⁴C. Cohen-Tannoudji and A. Kastler, Ref. 1, p. 50.